Applied Physics B (2018) 124:221
https://doi.org/10.1007/s00340-018-7090-y

Applied Physics B
Lasers and Optics

Diffraction-enhanced femtosecond white-light filaments in air

V. Vaičaitis[1] · R. Butkus[1] · O. Balachninaitė[1] · U. Morgner[2] · I. Babushkin[2]

Received: 22 May 2018 / Accepted: 25 October 2018 / Published online: 31 October 2018

Abstract
Here we demonstrate filamentation and generation of intense white light supercontinuum from a weakly focused femtosecond Ti:Sapphire laser pulses modified by a partial laser beam blocking by the knife edge. Though the spectral broadening of the filamented laser pulses was observed both in the blue and red sides of the fundamental wavelength, most distinct was the broadband white-light emission covering the whole visible spectral range. The dominant filamentation and supercontinuum generation enhancement mechanism was found to be the diffraction-induced laser beam intensity modification.

1 Introduction

Propagation of focused femtosecond laser pulses in air usually is accompanied by a variety of nonlinear optical phenomena, such as air ionization [1], third and fifth harmonic generation [1–4], four- and six-wave mixing [5, 6], self-focusing and filamentation, self-phase modulation, etc. [7, 8]. Under certain conditions, the spectral broadening of the propagating laser pulses may reach few octaves, i.e., generation of supercontinuum (SC) in the visible and infrared spectral regions takes place [9–14]. The SC may find many promising applications (remote sensing of the atmosphere and lightning control [9], generation of ultrashort laser pulses [10], time-resolved pump–probe spectroscopy [11], etc.); therefore, the control of its parameters is of major importance. Although SC can be produced in waveguides [15–18], the free-propagation-based SC not only allows, as a rule, significantly higher pulse energies [9–14] but also is subject of more complicated spatio-temporal dynamics that makes the control of SC in filaments a complicated task. To achieve this goal, the field gradients and phase changes on the input beam were introduced [19] or the beam astigmatism and ellipticity [20] were used. However, one of the most widespread methods to produce SC in a single filament remains a simple focusing of ultrashort laser pulses in a nonlinear medium. On the other hand, the diffraction of ultrashort pulses on the apertures of different shapes such as circular ones [21–23], slits [24] and knife edges [25, 26] has already been investigated. It was shown that the diffraction can cause not just a spatial beam modulation, but also the spectral and temporal pulse modifications [27, 28]. For instance, in [25, 26] it was shown that the diffraction on the knife edge induces a small-scale self-focusing, modulation instabilities and shock waves.

In this paper, we demonstrate for the first time that for a loosely focused femtosecond laser pulses in air, the partial beam blocking leads to more than one octave long SC generation. Note that in contrast to the spectrum generated by simply focused laser beam the spectral intensity of the SC generated by partially blocked laser beam was found to be at least an order of magnitude higher in the visible spectral range. We attribute the effect to nonlinearity-induced enhancement of diffraction on the edge leading to the onset of modulation instability and thus to spectral broadening.

2 Experimental

For the experiments we have used a 1 kHz repetition rate femtosecond Ti:sapphire chirped pulse amplification laser system (Legend elite duo HE+, Coherent Inc.), delivering 35–40 fs (FWHM) light pulses centered at 790 nm with a maximal pulse energy of 8 mJ, which could be varied by an attenuator composed of a zero-order half-wave plate and a broadband polarizer. The laser pulses were focused in air by a lens with the focal length of 100 cm and as a result a visible plasma filament of about 6 cm long was produced.

✉ V. Vaičaitis
Virgilijus.Vaicaitis@ff.vu.lt

[1] Laser Research Center, Vilnius University, Saulėtekio 10, Vilnius 10223, Lithuania

[2] Institute of Quantum Optics, Leibniz University of Hannover, D30167 Hannover, Germany

At about 60 cm from the lens (at this position the diffraction-induced SC generation was most efficient) part of the focused beam was fully or partially blocked by the edge of a metallic knife (Fig. 1). Near the knife edge, the laser beam diameter at FWHM was about 2.8 mm, while at the focusing lens it was about 6.5 mm (Fig. 2). The far-field patterns of the visible radiation generated in air by the laser pulses were observed on a white paper screen placed at about 3 m beyond the beam filament and registered with the help of a CCD camera. The spectra of this radiation have been registered with the help of a fiber spectrometer sensitive in the visible and NIR spectral ranges by placing its fiber input at the positions of the bright SC spots shown in Fig. 3.

3 Results and discussion

The typical far-field patterns of the visible radiation generated in air by the weakly focused laser pulses consisted of irregular yellow–red patterns with a small white–yellow spot

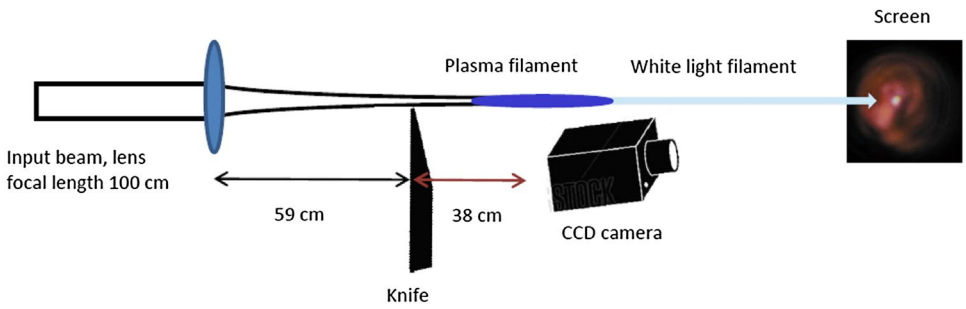

Fig. 1 Experimental setup

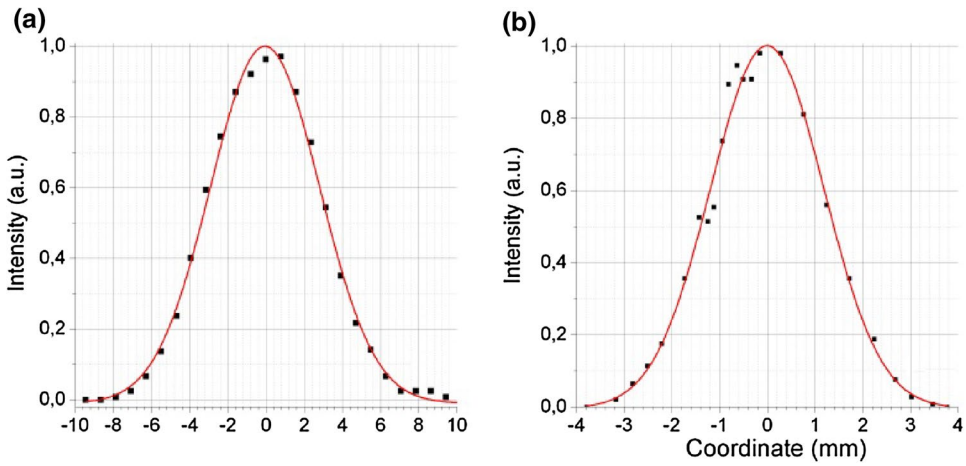

Fig. 2 Laser beam intensity profile **a** just before the focusing lens and **b** near the knife edge

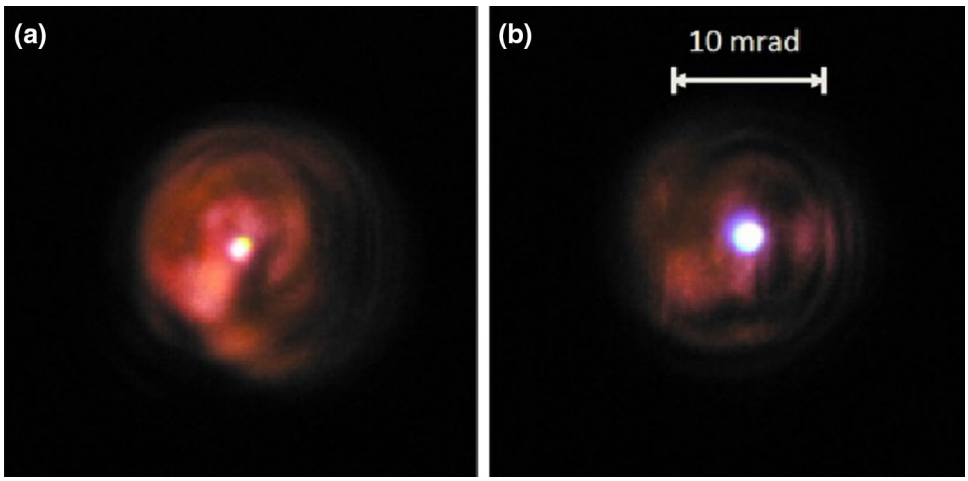

Fig. 3 Angular spectra of supercontinuum emitted from the filament formed by **a** weakly focused and by **b** partially blocked laser beam. The focal length of the focusing lens was 1 m in both cases, the distance from the plasma filament centre to the white screen was about 3 m, the diameter of the bright spot seen on the right panel was about 6 mm. The pulse duration was 40 fs, single pulse energies of the unblocked and partially blocked beams were about 3.4 and 3 mJ, respectively

in the centre, which could be seen at high (more than 3 mJ) laser pulse energies and apparently represents a SC generated upon the pulse propagation in air (Fig. 3a).

When the knife edge was moved across the beam blocking the pulse energy, the intensity of the yellow–red pattern (and white–yellow spot) first decreased a little but then (when about 10% beam power was blocked) the white–yellow spot disappeared and the new very bright white spot was formed (Fig. 3b). Note that at the same time, the intensity of the yellow–red surrounding emission decreased considerably. When more than 40% of the laser pulse energy was blocked, this white spot also disappeared and the intensity of the yellow–red patterns decreased along with decreasing of the transmitted pulse energy.

Furthermore, the spectral measurements revealed that in the visible range the spectral intensity of the white spot was at least an order of magnitude higher than that in the white–yellow spot generated by unperturbed laser beam (Fig. 4a). Note that though the spectrum of SC covered all the visible spectral range, the obvious spectral broadening to the red side of the laser wavelength was also observed (Fig. 4a). The possible reasons of the redshift (of both the perturbed and unperturbed beams) is the self-phase modulation (SPM) broadening [29]. Besides, as noticed in [25], modulation instability can develop, which may lead to additional spectral broadening in both sides of the spectrum. The blue cut-off wavelength of SC was close to 400 nm, which corresponds well to that obtained using tightly focused femtosecond laser pulses [30]. The spectral dynamics of SC as a function of the transmitted laser beam power (Fig. 4, right) allowed to define conditions of the white spot appearance: it has been registered, when from 10 to 40% of the beam power was blocked (or from 90 to 60% beam power transmitted). Note that the registered spectrum was practically the same as in the case of unperturbed beam when from 90 to 100% beam power was transmitted.

Note that when the laser beam was partially blocked and bright white spot was generated, the intensity of the plasma fluorescence significantly decreased (see Fig. 5), which indicates the lower plasma particle density and laser beam intensity inside the filament. However, even at the reduced light intensities inside the plasma filament at some distance from it (at the screen in our case) the bright SC spot is formed due to the diffraction-modified pulse propagation conditions, i.e., the spatial beam intensity redistributes forming a high light intensity region in the expense of the whole beam power. This fact may be explained assuming that the light diffraction from the knife edge modifies the intensity profile in the beam and thus the self-focusing and pulse propagation processes are modified, favoring weaker beam filamentation and, consequently, a longer high light intensity region along the pulse propagation axis (including the beam beyond the plasma filament).

Intensity of the plasma fluorescence as a function of the coordinate along the beam axis is shown in Fig. 6. One may see that the beam blocking practically does not

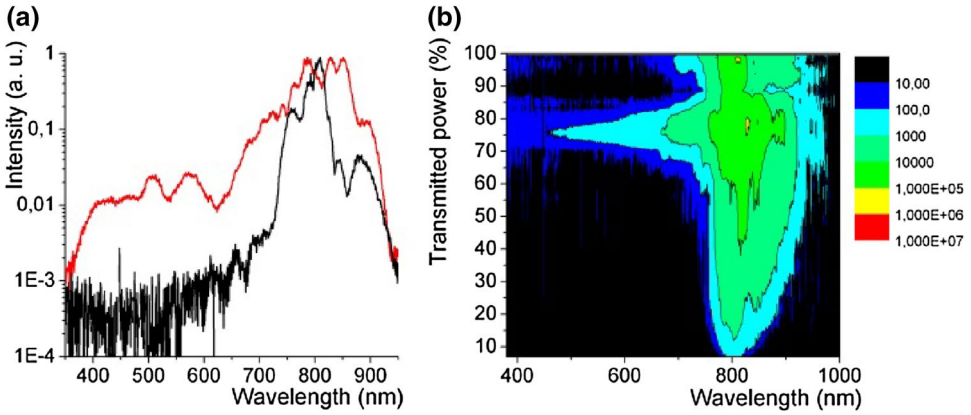

Fig. 4 **a** Spectra of the bright spots generated by unperturbed (black line) and partially blocked (red line) laser beams. **b** Spectral evolution of SC as a function of the transmitted laser beam power

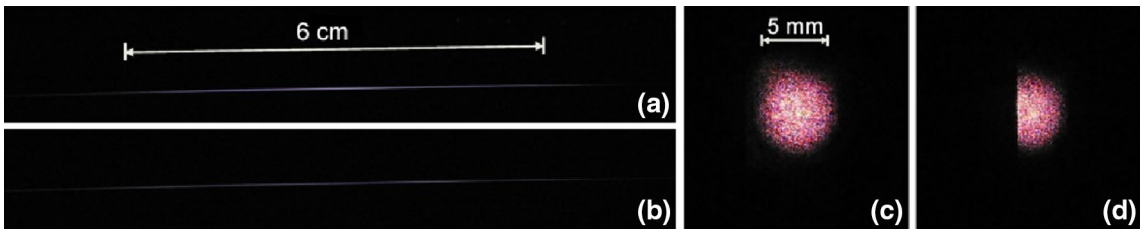

Fig. 5 (Left) Typical side views of the plasma filaments formed by the full (**a**) and partially blocked (**b**) laser beams. **c, d** Corresponding spatial intensity profiles of the beam transmitted after the knife edge

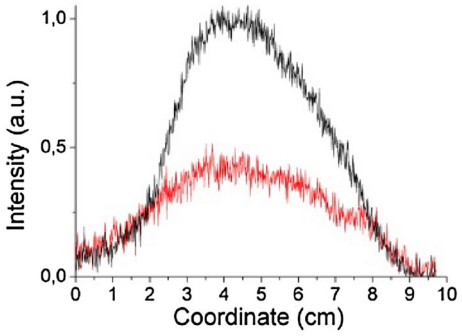

Fig. 6 Plasma fluorescence intensity in the filament as a function of the coordinate along the optical axis. Black line is fluorescence of the unblocked beam, while the red curve represents fluorescence from the filament created by the partially blocked pump

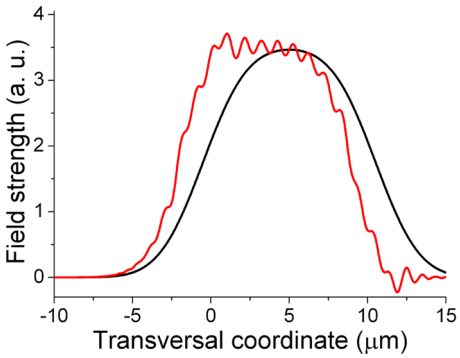

Fig. 7 Spatial distribution of the electric field strength in the case of unperturbed (black line) and partially blocked (red line) beams. Knife is blocking part of the beam at $x \leq 0$

influence the filament length and its onset position. However, Fig. 6 shows that the fluorescence intensity in the case of the partially blocked and unblocked beams are the same at the early stages of filament formation, but the maximal intensity is higher in the case of the unblocked beam.

Note that the broadband SC radiation could also be observed, when the knife was replaced with the variable circular aperture; however, in that case for the efficient SC generation the system transmission had to be slightly (by a few percent) reduced.

To get further look into this apparently contradictive behavior, we consider diffraction on the knife edge. Thus, the Fresnel diffraction produced by a focused laser beam short after the screen edge is described by [31]:

$$E(x,y,z) = \frac{-i}{\lambda}\int E(x',y',z')\frac{e^{ikr}}{r}\mathrm{d}x'\mathrm{d}y',$$

here λ is the wavelength, k is the corresponding wavevector and r is the distance between the points (x,y,z) and $(x',y',0)$. The corresponding distributions for a Gaussian beam with the diameter 10 μm are shown in Fig. 7 with the knife represented as a semiinfinite nontransparent screen placed at $x=0$ and covering negative values of x. The spatial intensity modulation seen in Fig. 7 significantly modifies the beam filamentation processes taking place after the knife. As one can see, the intensity modulations near the edge can even increase locally the beam intensity.

Thus, modification of the focusing conditions takes place. In addition, it was shown in [25, 26] that the optical nonlinearity leads to amplification of these modulations resulting in a spatial modulational instability (MI) and shock formation. It is known that temporal MI plays a key role in SC generation in waveguides [18, 32, 33]. In our case, the spatial MI can work at least as a trigger invoking more common mechanisms playing the role in SC formation in free filaments [7, 8, 34]. Besides, the temporal modulations may also appear due to the beam diffraction, which is intrinsicly frequency dependent [35]. As for SC generation in free filaments, most often the key player is the self-phase modulation (SPM) [7, 8, 34], although self-steepening and chromatic dispersion may also play an important role [36, 37]. However, the comprehensive modeling of the diffraction and SC generation including the temporal effects is a sophisticated task and is beyond the scope of our manuscript and will be a subject of further investigations.

4 Conclusions

In conclusion, we have demonstrated, for the first time, a diffraction-induced filamentation of a weakly focused femtosecond laser beam and formation of the more than one octave spanning supercontinuum. The SC generation efficiency in such diffraction-induced laser filament was found to be at least an order of magnitude higher than that obtained from a simply focused beam. The experimental results were interpreted in terms of nonlinearly modified Fresnel diffraction from the knife edge which leads to self-phase modulation and therefore to the spectral broadening.

Acknowlegements This project has received funding from the European Union's Horizon 2020 research and innovation programme under Grant agreement no 654148 Laserlab-Europe. IB and UM are thankful to financial support of DFG (MO 850-19/2, MO 850-20/1, BA 4156/4-2).

References

1. C. Rodriguez, Z. Sun, Z.Wang,W. Rudolph, Opt. Express **19**(17), 16115–16125 (2011)

2. G.O. Ariunbold, P. Polynkin, J.V. Moloney, Opt. Express **20**(2), 1662–1667 (2012)
3. V. Vaičaitis, Opt. Commun. **185**(1–3), 197–202 (2000)
4. J.A. Nath, A.K. Dharmadhikari, Dharmadhikar, D. Mathur, Opt. Lett. **38**(14), 2560–2562 (2013)
5. F. Théberge, N. Aközbek, W. Liu, A. Becker, S.L. Chin, Phys. Rev. Lett. **97**(2), 023904 (2006)
6. V. Vaičaitis, V. Jarutis, K. Steponkevičius, A. Stabinis, Phys. Rev. A **87**(6), 063825 (2013)
7. A. Couairon, A. Mysyrowicz, Phys. Rep. **441**(2–4), 47–189 (2007)
8. L. Bergé, S. Skupin, R. Nuter, J. Kasparian, J.-P. Wolf, Rep. Prog. Phys. **70**(10), 1633–1713 (2007)
9. J. Kasparian, M. Rodriguez, G. Méjean, J. Yu, E. Salmon, H. Wille, R. Bourayou, S. Frey, Y.B. Andre, A. Mysyrowicz, R. Sauerbrey, J.P. Wolf, L. Wöste, Science **301**(5629), 61–64 (2003)
10. B. Schenkel, J. Biegert, U. Keller, C. Vozzi, M. Nisoli, G. Sansone, S. Stagira, S. De Silvestri, O. Svelto, Opt. Lett. **28**(20), 1987–1989 (2003)
11. L. Dobryakov, S.A. Kovalenko, A. Weigel, J.L. Pérez-Lustres, J. Lange, A. Müller, N.P. Ernsting, Rev. Sci. Instrum. **81**(11), 113106 (2010)
12. C. Brée, I. Babushkin, U. Morgner, A. Demircan, Phys. Rev. Lett. **118**(16), 163901 (2017)
13. V. Mitrofanov, A.A. Voronin, D.A. Sidorov-Biryukov, S.I. Mitryukovsky, M.V. Rozhko, A. Pugžlys, A.B. Fedotov, V.Ya. Panchenko, A. Baltuška, A.M. Zheltikov, Opt. Lett. **41**(15), 3479–3482 (2016)
14. V. Vaičaitis, M. Kretschmar, R. Butkus, R. Grigonis, U. Morgner, A. Demircan, I. Babushkin, J. Phys. B: At. Mol. Opt. Phys. **51**, 045402 (2018)
15. J.M. Dudley, G. Genty, S. Coen, Rev. Mod. Phys. **78**(4), 1135–1184 (2006)
16. V. Husakou, J. Herrmann, Phys. Rev. Lett. **87**(20), 203901 (2001)
17. J.M. Dudley, J.R. Taylor, Ten years of nonlinear optics in photonic crystal fibre. Nat. Photonics **3**(2), 85–90 (2009)
18. I. Babushkin, A. Tajalli, H. Sayinc, U. Morgner, G. Steinmeyer, A. Demircan, Light Sci. Appl. **6**, e16218 (2017)
19. G. Méchain, A. Couairon, M. Franco, B. Prade, A. Mysyrowicz, Phys. Rev. Lett. **93**(3), 035003 (2004)
20. G. Fibich, S. Eisenmann, B. Ilan, A. Zigler, Opt. Lett. **29**(15), 1772–1774 (2004)
21. K. Cook, A.K. Kar, R.A. Lamb, Opt. Express **13**(6), 2025–2031 (2005)
22. M. Lefrançois, S.F. Pereira, Opt.Express **11**(10), 1114–1122 (2003)
23. D. He, Z. Liu, Y. Jiang, J. Mod. Opt. **62**(8), 620–625 (2015)
24. R. Netz, T. Feurer, Appl. Phys. B **70**(6), 813–819 (2000)
25. W. Wan, D.V. Dylov, C. Barsi, J.W. Fleischer, Opt. Lett. **35**(16), 2819–2821 (2010)
26. N. Wang, C. Tan, X. Fu, Opt. Quant. Electron. **47**(8), 2697–2707 (2015)
27. O. Mendoza-Yero, G. Mínguez-Vega, J. Lancis, M. Fernández-Alonso, V. Climent, Opt. Express **15**(8), 4546–4556 (2007)
28. O. Mendoza-Yero, B. Alonso, O. Varela, G. Mínguez-Vega, Í Juan Sola, J. Lancis, V. Climent, L. Roso, Opt. Express **18**(20), 20900–20911 (2010)
29. L. Ahmad, Z. Bergé, F. Major, S. Krausz, Karsch, S.A. Trushin, New J. Phys. **13**, 093005 (2011)
30. X.-L. Liu, X. Lu, X. Liu, L.-B. Feng, J.-L. Ma, Y.-T. Li, L.-M. Chen, Q.-L. Dong, W.-M. Wang, Z.-H. Wang, Z.-Y. Wei, Z.-M. Sheng, J. Zhang, Opt. Lett. **36**(19), 3900–3902 (2011)
31. G.D. Durgin, IEEE Antennas Propag. Mag. **51**(3), 24–35 (2009)
32. A. Demircan, U. Bandelow, Opt. Commun. **244**(1), 181 (2005)
33. M. Dudley, J.R. Taylor, Nat. Photonics **3**, 85 (2009)
34. R. Kasparian, D. Sauerbrey, S. Mondelain, J. Niedermeier, J.P. Yu, Y.-B. Wolf, M. André, B. Franco, S. Prade, M. Tzortzakis, H. Rodriguez, Wille, L. Wöste, A. Mysyrowicz, Opt. Lett. **25**, 1397 (2000)
35. S.P. Veetil, C. Vijayan, D.K. Sharma, H. Schimmel, F. Wirowski, J. Modern Opt. **53**, 1819 (2005)
36. N. Aközbek, M. Scalora, C.M. Bowden, S.L. Chin, Opt. Commun. **191**, 353 (2001)
37. M. Kolesik, G. Moloney, J.V. Katona, E.M. Wright, Appl. Phys. B **77**, 185 (2003)